Available online at www.sciencedirect.com

ScienceDirect

Procedia Structural Integrity 2 (2016) 3337–3344

Structural Integrity Procedia

www.elsevier.com/locate/procedia

21st European Conference on Fracture, ECF21, 20-24 June 2016, Catania, Italy

Influence Yield Stress on Arrest Pressure in Pipe Predicted by CTOA

M.Benamara[a], G.Pluvinage[b], J.Capelle[a], Z.Azari[a]*

[a]LaBPS – ENIM, 1 route d'Ars Laquenexy, CS 65820, Metz 57078, France
[b]FM.C Silly Sur-Nied 57530, France

Abstract
In this paper, the resistance to ductile crack extension is discussed in terms CTOA. Selection of CTOA is based on the reduced number of parameters and the low sensitivity to pipe geometry. Numerical simulations of crack propagation and arrest based on CTOA use the node release technique, which is described. Results on a pipe made in steel API L ,X52, X65 and X 100 are presented. The influence material parameters on crack arrest and velocity using this technique are presented. For the same decompression wave pressure, the crack propagation velocity is inversely proportional to the resistance to crack extension of the material, which is the dominant parameter. The crack velocity versus decompression is expressed by a $CTOA_c$ function of resistance to crack extension

Peer-review under responsibility of the Scientific Committee of ECF21.

Keywords: CTOA; pipe steels; crack arrest; crack extension;

1. Introduction

One of the objectives of the pipe design is to reduce the crack arrest length in order to repair within a reasonable cost. To solve this problem, developing relationships are required between the decompression behaviour, arrest stress level, and fracture velocity.

The basic idea is to compare fracture resistance and driving force during crack extension. Immediately, when a trough crack appears at the surface of the wall of the pipeline, the gas tends to escape through the opening plug created. This leads to a sudden decompression and creation of two opposite decompression waves running at a speed

* Corresponding author.
E-mail address: pluvinage@cegetel.net

Peer review under responsibility of the Scientific Committee of ECF21.
10.1016/j.prostr.2016.06.416

of the order of 300 m/s along the main direction of the pipe. These waves play the major role on the dynamics of pipe fracture. If the decompression wave celerity is less than the crack propagation speed, the crack tip is constantly loaded at initial pressure, inducing stationary crack propagation. On the contrary, the crack is progressively less unloaded until arrest.
In this paper, we propose to use the crack tip opening angle (CTOA) as a measure of fracture resistance and using a simplified gas depressurisation model, where gas pressure is a function of time and distance from the crack tip. Examples of prediction of arrest pressure and length are given in the case of a pipe of 355 mm diameter and 19 mm wall thickness, made in pipe steel API5L X 65.The influence of material parameters on crack arrest and crack velocity is discussed.

2. Numerical simulation of crack propagation and arrest based on CTOA

Conditions for crack propagation or arrest are given by a coupled fluid-structure problem. Crack propagation speed is controlled by pressure distribution on the opening pipe. If the decompression wave is faster than the propagating crack fracture, the pressure at crack tip will decrease, and the crack will arrest.
In terms of a limit state design, the arrest pressure can be predicted by solving the Equation (1) between the fracture resistance and component stress, which depend on the pipeline dimensions, internal pressure and material strength. This material resistance is balanced with a component stressing that is determined involving specific pipe dimensions, decompression pressure p_d and material strength. The arrest pressure can be predicted by solving the equation between the stress state at crack tip :

$$\langle \sigma_{ij}(\, p_d)\rangle = \langle \sigma_{ij,c}(p_{ar})\rangle \tag{1}$$

In principle, to solve the gas depressurisation problem, one has to solve a coupled gas-solid thermomechanical problem. There are specialised codes developed for this purpose, e.g. GASDECOM (Eiber et al,1993).
Generally simplified gas depressurisation models have been proposed in literature, which only predict gas pressure as a function of time and distance from the crack tip. These models are based on the isentropic expansion of ideal gas, where a pipe is considered a large pressure vessel with constant volume. These assumptions are justified by the fact that crack propagation cannot outrun the decompression wave. This means that the crack tip is always present in pipe section affected by the decompression process. Gas pressure ahead of the crack depends only on time. This simplification is justified by the fact that the crack propagation speed is at most 200–300 m/s, which is lower than the wave speed in the pressurized gas, estimated at about 400 m/s. This means that the crack cannot outrun the pressure drop wave, and the crack tip will always be in a segment of the pipe with falling pressure. The drop pressure ahead of the running crack tip is given as:

$$p_d(t) = p_0.\exp(kt) \tag{2}$$

k is a constant expressed as:

$$k = -\frac{A}{V_0}\sqrt{\frac{RT}{W_g}} \tag{3}$$

where A is the cross-sectional area of the pipe, V_0 is the initial volume, R is the universal gas constant, T is the average temperature of the gas and W_g is the molecular weight of the gas, k = -7.5 (Eiber et al,1993).
Instantaneous internal pipe pressure was imposed along a certain distance behind the crack-tip node: Fig. 6. This distance was given by the cohesive zone model of Dugdale-Barenblatt (Maxey , 1981) The distance is $2b = 3\sqrt{R.t}$, where R and t are outer radius and wall thickness, respectively Fig.1.
Pressure drop behind the crack tip is expressed only as a function of distance. For distances exceeding 1.75 pipe diameters behind the crack tip, the pressure is considered zero. It is also possible to assume a linear pressure drop behind the running crack tip (Oikonomidis et al, 2013):

$$p_b(z) = p_0\left(1 - \frac{z}{1.75D}\right) \tag{4}$$

where $p_b(z,t)$ is the gas pressure behind the crack tip, which is a function of the distance z, and of time t and p_0 is the initial gas pressure prior to the appearance of the through thickness crack.
The use of CTOA to model the ductile crack propagation of thin structures has been validated by several authors [Demofonti et al, 1995]. To simulate crack propagation, the CTOA fracture criterion is introduced in a numerical model using the node release technique. Condition of node release is given by the following equation:

$$CTOA\ (p_{ar}) = CTOA_c \tag{5}$$

where CTOA is the crack tip opening angle induced by the current pressure, p_{ar} the arrest pressure and $CTOA_c$ the fracture resistance.
The node release technique is based on the assumption that the crack growth is described by uncoupling nodes at the crack faces, whose acting tractions are reduced as far as the crack opens. When the CTOA reaches its critical value ($\Psi = \Psi_c$), the representative node of the crack tip is released and a new position of the crack is deduced. Each propagation step corresponds to the size of a mesh element (see Fig. 1). In this method, crack evolution depends on the size of mesh elements around the crack tip, since it governs the amount of the crack advance. Moreover, the advancing process is not really continuous, since a proper iteration scheme is necessary to evaluate the dynamic crack growth during the integration time accurately.
The method requires an a priori knowledge of the crack propagation path. The simulation is performed on a pipe with an outer diameter of 355 mm, wall thickness of 19 mm, and length of 6 m. The studied pipe is made of API 5L X65 steel with a critical CTOA value of 20° (Ben Amarra et al, 2015).
The computing phase begins by generating a 3D finite element implicit dynamic analysis. Because of the symmetry of the crack planes, only a quarter of the pipeline was analysed. A combined 3D-shell mesh was used to reduce the computing time. A total of 50976 eight-node hexahedral elements were generated along the crack path and combined with 6000 shell elements.

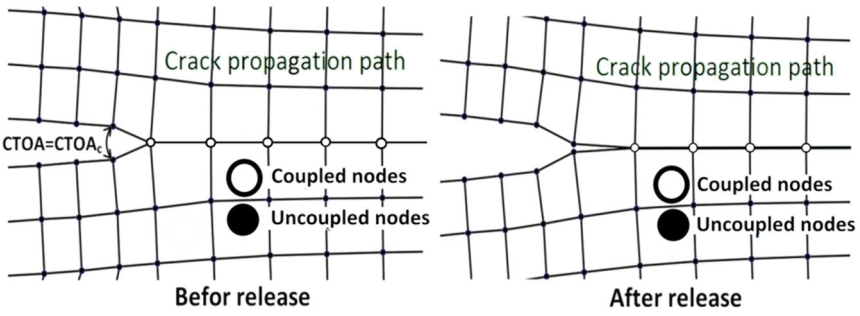

Fig. 1. Crack propagation according to the node release technique and the CTOA criterion, mode I and 2D.

Crack arrest in gas pipelines was performed with the release user subroutine, in conjunction with the FEM ABAQUS code. The computing phase begins by generating a 3D finite element implicit dynamic analysis. Because of the symmetry of the crack planes, only a quarter of the pipeline was analysed.
Crack extension from an initial crack-like defect is computed using the described model. Running crack propagation along the tube consists of two stages: a boost phase, where the crack reaches its full velocity in a few milliseconds, followed by a steady stage at constant speed. The absence of a deceleration phase is explained by the absence of a pressure drop.
The crack velocity increases with the initial pressure. Ten simulations were performed at different levels of pressure in the range of 28–60 MPa (Fig.2).
The results indicate that the stationary crack velocity V_c [m/s] increases with initial pressure p_0 [MPa] according to:

$$V_c = 284.2 * (\frac{p_d}{25.8} - 1)^{0.193} \tag{6}$$

p_0 has been replaced by decompression pressure because if $V_c > V_d$ $p_0 = p_d$
Qualitatively, this equation is consistent with the experimental results reported by Battelle, HLP, and many other

authors (Maxey ,1974, Sugie et al, 1982, Higuchi et al, 2009). Crack extension at arrest is obtained from the graph of crack velocity versus half the crack extension, to take into account the symmetry of the problem. For the aforementioned conditions of geometry, material, and initial pressure, the numerical simulation gives a crack extension of 42 m, which is of the same order of magnitude as those obtained experimentally.

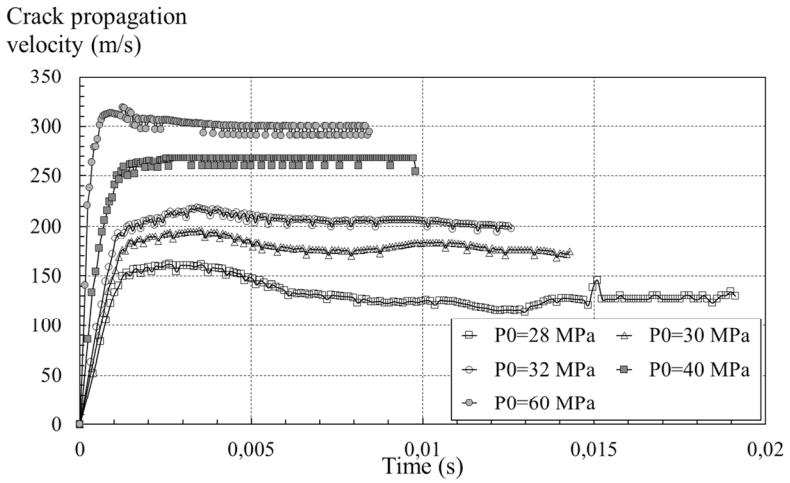

Fig. 2. Crack velocity pipe versus time for different initial pressure in API 5L X65, diameter 355 mm and thickness 19 mm.

3. Influence of geometrical and material parameters on crack arrest and velocity

Prediction of crack arrest and crack velocity after fracture initiation in a pipe submitted to internal pressure is modelled here using critical CTOA as a parameter representative of the fracture resistance to crack extension R_f. This parameter is sensitive to geometry in general and to diameter and thickness for pipe particularly. It is also sensitive to material through its flow stress σ_0.

The influence of these different parameters on CTOA has been described by (Demofonti et al,2004) and is given by the general form*:*

$$CTOA \quad = C\left(\frac{\sigma_h}{E}\right)^m \left(\frac{\sigma_h}{\sigma_0}\right)^n \left(\frac{D}{t}\right)^q \tag{7}$$

where m, n, and q are dimensionless constants and C is expressed in degrees; σ_h is the hoop stress (MPa), σ_0 is the flow stress (MPa), D is the diameter (mm), and t is thickness (mm). The following values can be used for methane: C = 106, m = 0.753, n = 0. and q = 0.65. Influence of the quantities $\sqrt{Dt}$ on initial pressure p_0 is introduced by through the Folias factor (Maxey ,1974):

$$p_0 = \sigma_h \frac{2t}{D} = \frac{\sigma_0}{M_F}.\frac{2t}{D} \tag{8}$$

where M_F is the Folias correction factor :

$$M_F = \left[1 + 1.255.\left(\frac{a}{\sqrt{Dt/2}}\right)^2 - 0.0135.\left(\frac{a}{\sqrt{Dt/2}}\right)^4\right]^{1/2} \tag{9}$$

3.1 Influence of thickness

Arrest pressure and crack velocity have been computed using the aforementioned node release technique with four different pipe wall thicknesses [5, 10, 15, 19.05 mm]. In each case, the pipe has a diameter of 355 mm and is made

of steel API 5L X65 with a yield stress equal to 465 MPa. Results are reported in Figs. 3 and 4.

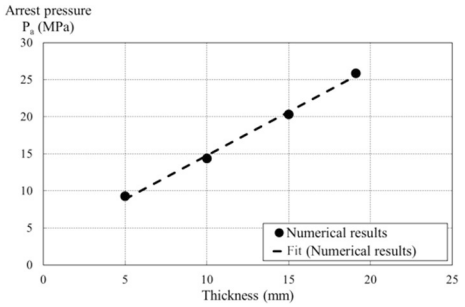

Fig. 3. Influence of pipe wall thickness on arrest pressure, pipe diameter 355 mm ,steel API 5L X65, yield stress 465 MPa.

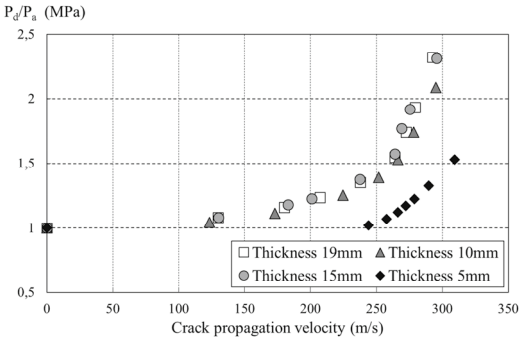

Fig. 4. Influence of pipe wall thickness on crack velocity, pipe diameter 355 mm ,steel API 5L X65, yield stress 465 MPa.

Fig.3 shows a linear evolution between arrest pressure and wall thickness. On Fig. 4, the ratio of decompression wave and arrest pressure is plotted versus the crack velocity for the four studied wall thicknesses. The velocity obeys the general law:

$$V_c = H \,.\left(\frac{p_d}{p_a} - 1\right)^{\beta} \tag{10}$$

where H is a material constant that depends on initial pressure, flow stress and resistance to crack extension of the material, β another constant. There is no influence of wall thickness for values above 10 mm. Higher velocities for low values of the wall thickness may be the result of a mesh problem without certainty. However a wall thickness of 5 mm for a pipe of 355 mm of diameter is not realistic and generally wall thickness for a gas pipe is over 8 mm.

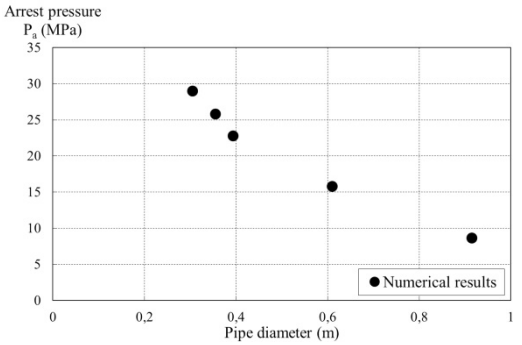

Fig. 5. Influence of pipe diameter on arrest pressure, pipe thickness 19 mm, steel API 5L X65, yield stress 465 MPa.

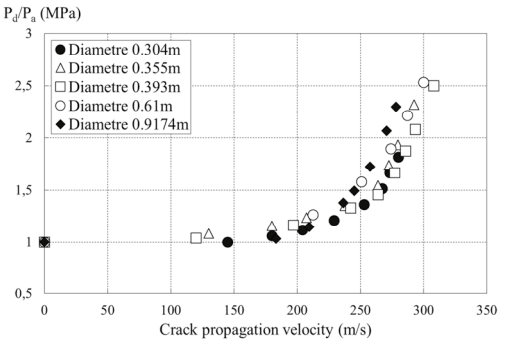

Fig. 6. Influence of pipe diameter on crack velocity, pipe thickness 19 mm, steel API 5L X65, yield stress 465 MPa.

Five simulations to study the influence of the diameter on crack velocity and arrest pressure have been performed. The pipe thickness has been chosen as 19.05 mm and pipe diameter as 0.304, 0.355, 0.393, 0.61 and 0.91 m. The evolutions of arrest pressure and crack velocity pressure have been plotted versus the pipe diameter: Figs. 5 and 6. We notice that the arrest pressure is a decreasing function of the diameter of the pipeline. We also highlight a minor effect of the pipe diameter on crack velocity.

3.2 Influence of yield stress

Several simulations of pipe bursting have been made on three pipe steels API 5L X46 with a yield stress σ_y =. 320 MPa, API 5L X65 with σ_y = 465 MPa and API 5L X100 with σ_y =735 MPa keeping the other parameters identical,

i.e., the geometry of the pipe, the strain hardening and the mesh size. The arrest pressure has been computed using the the node release technique and for different values of CTOA in the range 5-20°. Results are presented in Fig.7. One notes that for a given value of the yield stress, the arrest pressure increases with CTOA values rapidly for CTOA values less than 10 ° and slowly above these values. An asymptotic values is obtained in the range of CTOA [13-20°]. These results indicate that for the usual range of CTOA for pipe steel, any error on CTOA determination has a little influence on arrest pressure. The arrest pressure at asymptotic value increases with the yield stress according to:

$$p_a\,(\text{MPa}) = 0.0363\ \text{CTOA}\,(°) + 8.2 \tag{11}$$

This increases of the arrest pressure with yield stress is due to the necessary plasticity and damage for the ductile crack extension which naturally occurs at higher pressure when yield stress increases. Several values of CTOA, for pipe steels indicates that critical CTOA ψ_c increases with yield stress according to:

$$\psi_c\,(°) = 0.0131\sigma_y\,(\text{MPa}) + 4.1 \tag{12}$$

The critical value of CTOA for each steel has been reported on figure 7 and the corresponding arrest pressures $p_a(\psi_c)$ are extracted. Equ.25 indicates a linear relationship between $p_a(\psi_c)$ and the yield stress σ_y

$$p_a\,(\psi_c) = 0.04\ \sigma_y\,(\text{MPa}) + 5.4 \tag{13}$$

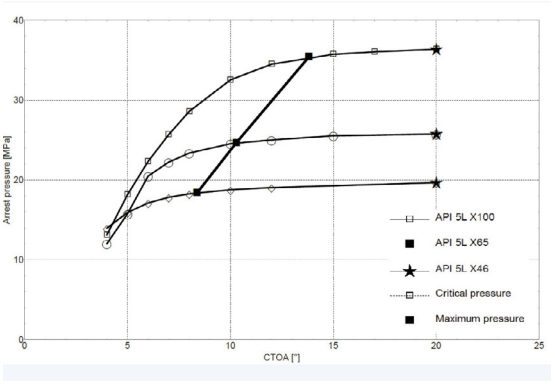

Fig. 7. Influence of yield stress on arrest pressure, pipe thickness 19 mm pipe diameter 355 mm , steel API 5L X6.5

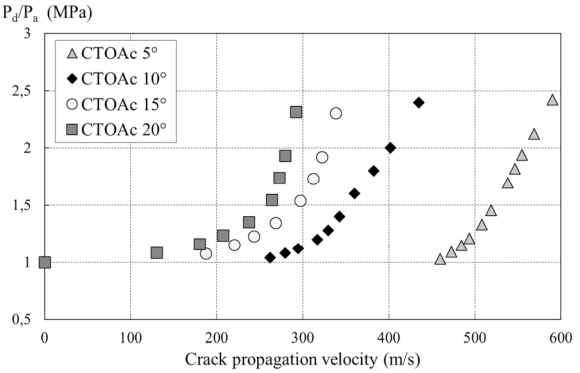

Fig. 8. Influence of CTOA on crack velocity pipe thickness 19 mm pipe diameter 355 mm, steel API 5L X65.

Influence of the resistance to crack extension has been studied, over 40 simulations keeping all the parameters of the numerical model identical. Only the value of $CTOA_c$ was modified in the range 5–20 °. Simulations of static and dynamic type provide the evolution of and crack velocity versus the resistance to crack extension, expressed in terms of CTOA Figs. 8 In Fig. 8, we notice an increase of the crack velocity with increasing CTOA. These results are consistent with the fact that the increases of the yield stress result in a decrease in toughness and therefore the resistance to crack extension.

3.3Arrest pressure equation

The arrest pressure is expressed by the following general equation, according to the BTCM (Maxey ,1974), HLP (Sugie et al, 1982) and HLP-Sumitomo (Higuchi et al, 2009) methods.

$$p_a = A.\frac{t}{D}.\sigma_0.cos^{-1}exp\left(\frac{-.\pi E.R_f}{24\sigma_0^2\sqrt{Dt/2}}\right) \tag{14}$$

A is a parameter that depends of the ratio diameter-thickness D/t. The arrest pressure is a linear function of the flow stress, which is confirmed by the numerical results. In the BTCM, the flow stress is defined as :

$$\sigma_0 = \sigma_y + 69\ MPa \tag{15}$$

Pipe made in API 5L X65 steel, pipe diameter 355 mm, thickness 19 mm. To take into account the strain hardening, the following definition is used:

$$\sigma_0 = (\sigma_y + \sigma_u)/2 \tag{16}$$

The arrest stress is defined as:

$$\sigma_a = \frac{p_a D}{2t} \tag{17}$$

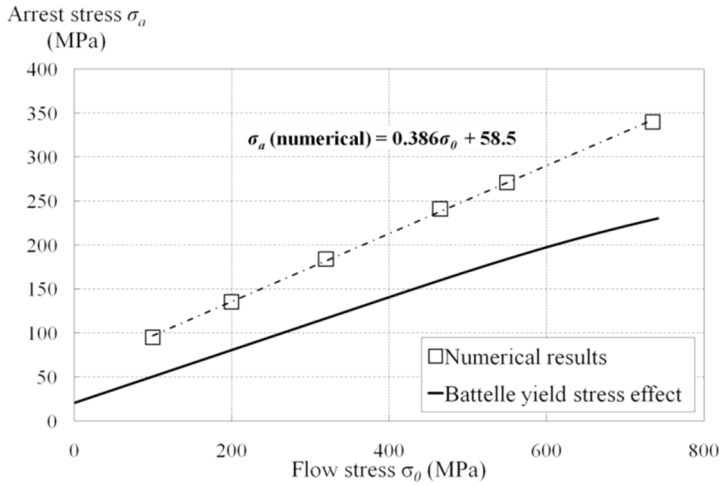

Fig. 9. Numerical simulation of arrest pressure versus flow stress using CTOA as resistance to crack extension.

In Fig. 9, the arrest stress has been plotted versus yield stress. Numerical simulations confirm the linear dependence of the arrest stress with the flow stress.

Several burst tests carried out at Batelle have been reported by Kiefner et al (Kiefner et al , 1972). They concern ductile fracture initiation, propagation and arrest in cylindrical vessels that range from 168–1219 mm and made in steel with yield stress in the range 151– 765 MPa. For these tests, the ratio of arrest stress and flow stress is plotted versus the parameter $\frac{.\pi E.CTOA_c}{24\sigma_0^2\sqrt{Dt/2}}$.

The arrest pressure curve separates the arrest zone with data as a triangle to crack extension zone with data as square. The flow stress according to Equation (28) is equal to 511 MPa and the ratio D/t =18.7. The best fit confirms the ($\cos^{-1}$exp) dependence of the arrest pressure with the parameter $\frac{\pi E.CTOA_c}{24\sigma_0^2\sqrt{Dt/2}}$ with the following equation, similar to the BTCM's equation with Ω and μ as another constants (Ω = 1.39, μ =115*10^3)

$$p_a = \Omega.\frac{t}{D}.\sigma_0.cos^{-1}exp\left(\frac{-\mu.\pi E.CTOA_c}{24\sigma_0^2\sqrt{Dt/2}}\right) \tag{18}$$

Conclusion

CTOA gives a good description of the resistance to crack extension due to its definition as the slope of the crack driving force in terms of COD versus crack extension. Therefore, this parameter is more appropriate than Charpy or DWTT energies which incorporate a part of energy for fracture initiation. Numerical simulation of crack extension

using CTOA is more appropriate that numerical simulations using : a dissipative energy with the cohesive zone model (CZM) (Scheider et al ,2006) ,a critical damage with the Gurson-Tvergaard-Needleman model (GTN) (Scheider et al ,2006) critical damage given by SRDD model (Oikonomidis et al, 2014) because only one material parameter is necessary . However it has been noted that predictions of crack velocity and arrest pressure depend on the geometry of the pipe and material yield stress. Therefore, it seems necessary to use a two parameters fracture Mechanics approach resistance to crack extension- constraint as CTOA-T or CTOA-A_2.

For the same decompression wave pressure, the crack propagation velocity is inversely proportional to the resistance to crack extension of the material, which is the dominant parameter. The crack velocity versus decompression is expressed by a $CTOA_c$ function versus the parameter $\frac{\pi E.CTOA_c}{24\sigma_0^2\sqrt{Dt/2}}$.

References

Ben amara, M., Capelle, J., Azari, Z., Pluvinage, G., 2015. Prediction of arrest pressure in pipe based on CTOA; Journal of pipe and Engineering, December .

Demofonti, G., Buzzichelli, G., Venzi, S., Kanninen, M., 1995. Step by step procedure for the two specimen CTOA test. In: Denys R (ed.). Pipeline Technology, vol II. Elsevier.G

Demofonti, G., Mannucci, G., Hillenbrand, H.G., Harris, D., 2004. Evaluation of X100 steel pipes for high pressure gas transportation pipelines by full scale tests. Int. Pipeline Conf., Calgary, Canada.

Eiber, R., Bubenik, T., Maxey, W., 1993. GASDECOM, computer code for the calculation of gas decompression speed that is included in fracture control technology for natural gas pipelines. NG-18 Report 208, American Gas Association Catalog.

Higuchi, R., Makino, H., Takeuchi, I., 2009. New concept and test method on running ductile fracture arrest for high pressure gas pipeline. In: 24th World Gas Conf., WGC 2009, Vol. 4, International Gas Union, Buenos Aires, Argentina, 2730–2737.

Kiefner, J.F., Eiber, R.J., Duffy, A.R, 1972. Ductile fracture initiation, propagation and arrest in cylindrical vessels. ASTM STP, 514 pp70–81.

Maxey, W. A., 1974. 5th Symp. on Line Pipe Research, PRCI Catalog No. L30174, Paper J, 16

Maxey, W.A, 1981. Dynamic crack propagation in line pipe, In: Analytical and Experimental, Fracture Mechanics, ed. Sih G.C and Mirabile M, 109-123.

Oikonomidis, F., Shterenlikht, A., Truman, C.E., 2013. Prediction of crack propagation and arrest in X100 natural gas transmission pipelines with the strain rate dependent damage model. part 1 : A novel specimen for the measurement of high strain rate fracture properties and validation of the SRDD model parameters. International Journal of Pressure Vessels and Piping 105, 60–68.

Scheider, I., Schödel, M., Brocks, W., Schönfeld, W., 2006. Crack propagation analyses with CTOA and cohesive model : Comparison and experimental validation. Engineering Fracture Mechanics 73(2), 252–263,

Sugie, E., Matsuoka, M., Akiyama, H., Mimura, T., Kawaguchi, Y., 1982. A study of shear crack-propagation in gas-pressurized pipelines, J. Press. Vess. – T. ASME 104(4), 338–343.